

# UC Irvine

## UC Irvine Previously Published Works

### Title

Kcne2 deletion impairs insulin secretion and causes type 2 diabetes mellitus

### Permalink

<https://escholarship.org/uc/item/62f0m6gm>

### Journal

The FASEB Journal, 31(6)

### ISSN

0892-6638

### Authors

Lee, Soo Min  
Baik, Jasmine  
Nguyen, Dara  
et al.

### Publication Date

2017-06-01

### DOI

10.1096/fj.201601347

### Copyright Information

This work is made available under the terms of a Creative Commons Attribution License, available at <https://creativecommons.org/licenses/by/4.0/>

Peer reviewed

# Kcne2 deletion impairs insulin secretion and causes type 2 diabetes mellitus

Soo Min Lee,\* Jasmine Baik,\* Dara Nguyen,\* Victoria Nguyen,\* Shiwei Liu,\* Zhaoyang Hu,<sup>†</sup> and Geoffrey W. Abbott\*<sup>1</sup>

\*Bioelectricity Laboratory, Department of Pharmacology and Department of Physiology and Biophysics, School of Medicine, University of California, Irvine, Irvine, California, USA; and <sup>†</sup>Laboratory of Anesthesiology and Critical Care Medicine, Translational Neuroscience Center, West China Hospital, Sichuan University, Chengdu, China

**ABSTRACT:** Type 2 diabetes mellitus (T2DM) represents a rapidly increasing threat to global public health. T2DM arises largely from obesity, poor diet, and lack of exercise, but it also involves genetic predisposition. Here we report that the KCNE2 potassium channel transmembrane regulatory subunit is expressed in human and mouse pancreatic  $\beta$  cells. *Kcne2* deletion in mice impaired glucose tolerance as early as 5 wk of age in pups fed a Western diet, ultimately causing diabetes. In adult mice fed normal chow, skeletal muscle expression of insulin receptor  $\beta$  and insulin receptor substrate 1 were down-regulated 2-fold by *Kcne2* deletion, characteristic of T2DM. *Kcne2* deletion also caused extensive pancreatic transcriptome changes consistent with facets of T2DM, including endoplasmic reticulum stress, inflammation, and hyperproliferation. *Kcne2* deletion impaired  $\beta$ -cell insulin secretion *in vitro* up to 8-fold and diminished  $\beta$ -cell peak outward  $K^+$  current at positive membrane potentials, but also left-shifted its voltage dependence and slowed inactivation. Interestingly, we also observed an aging-dependent reduction in  $\beta$ -cell outward currents in both *Kcne2*<sup>+/+</sup> and *Kcne2*<sup>-/-</sup> mice. Our results demonstrate that KCNE2 is required for normal  $\beta$ -cell electrical activity and insulin secretion, and that *Kcne2* deletion causes T2DM. KCNE2 may regulate multiple  $K^+$  channels in  $\beta$  cells, including the T2DM-linked KCNQ1 potassium channel  $\alpha$  subunit.—Lee, S. M., Baik, J., Nguyen, D., Nguyen, V., Liu, S., Hu, Z., Abbott, G. W. *Kcne2* deletion impairs insulin secretion and causes type 2 diabetes mellitus. *FASEB J.* 31, 2674–2685 (2017). www.fasebj.org

**KEY WORDS:** KCNQ1 ·  $K_v1.5$  ·  $K_v2.1$  · potassium channel

Type 2 diabetes mellitus (T2DM) prevalence is increasing globally, in large part as a result of alterations in lifestyle, including poor diet and lack of exercise. T2DM is thus often part of a larger syndrome, termed metabolic syndrome, which often includes obesity, hypertension, nonalcoholic fatty liver disease (NAFLD), hypercholesterolemia, and coronary artery disease (1). However, not all individuals with T2DM are obese, and there are other contributing factors, including genetic predisposition. For example, many studies have shown that inherited polymorphisms in *KCNQ1*, which encodes a voltage-gated potassium

( $K_v$ ) channel pore-forming ( $\alpha$ ) subunit, predispose to T2DM (2).

Unlike type 1 diabetes, which is predominantly genetically acquired and arises from immune attack and destruction of pancreatic insulin-secreting  $\beta$  cells, in T2DM the  $\beta$  cells are present but cannot secrete sufficient insulin to control blood glucose levels. T2DM is a balance between insufficient insulin secretion and insulin resistance, with the relative deficiencies in insulin secretion and sensitivity varying between individuals (3, 4). Insulin resistance alone is not sufficient to cause diabetes; it must be combined with inadequate insulin secretion (5–7).

Various potassium channels play roles in  $\beta$ -cell function and insulin secretion. The best-characterized in these respects is the  $K_{ATP}$  channel.  $K_{ATP}$  channels are each formed from an octamer of 2 types of subunits, a tetramer of Kir6.2  $\alpha$  subunits that spans the plasma membrane and forms the pore, and a tetramer of sulfonylurea receptors that facilitates sensing of the metabolic state of  $\beta$  cells by the channel complex. Increased blood glucose raises intracellular ATP levels in  $\beta$  cells. Intracellular ATP binds to the sulfonylurea receptors, resulting in inhibition of the  $K_{ATP}$  channel. Because  $K_{ATP}$  channels are weak inward rectifiers that are open

**ABBREVIATIONS:** APP, amyloid precursor protein; DEG, differentially expressed gene; ER, endoplasmic reticulum; GAPDH, glyceraldehyde-3-phosphate dehydrogenase; IRS-1, insulin receptor substrate 1; IR- $\beta$ , insulin receptor  $\beta$ ; KRB, Krebs-Ringer bicarbonate;  $K_v$ , voltage-gated potassium; NAFLD, nonalcoholic fatty liver disease; qPCR, quantitative PCR; T2DM, type 2 diabetes mellitus; TBST, Tris-buffered saline with 1% Tween-20

<sup>1</sup> Correspondence: University of California, Irvine, 360 Med Surge II, Medical School, Irvine, CA 92697, USA. E-mail: abbottg@uci.edu

doi: 10.1096/fj.201601347

This article includes supplemental data. Please visit <http://www.fasebj.org> to obtain this information.

at resting membrane potential, their inhibition initiates cellular depolarization. This opens  $\beta$ -cell voltage-gated  $\text{Ca}^{2+}$  channels, raising intracellular  $\text{Ca}^{2+}$  levels, signaling to the cell to secrete insulin. The insulin signals to the liver to stop releasing glucose into the blood and signals to skeletal muscle to take up glucose from the blood (8, 9). Inherited mutations in the genes encoding  $\text{K}_{\text{ATP}}$  channel subunits can contribute to diabetes. Mutations that moderately increase  $\text{K}_{\text{ATP}}$  channel activity can predispose to T2DM in adults; those that dramatically increase  $\text{K}_{\text{ATP}}$  channel activity, to the extent that glucose-dependent insulin secretion is essentially prevented, can cause syndromic neonatal diabetes (10).

Several  $\text{K}_v$  channels are also expressed in  $\beta$  cells and are involved in the repolarization phase of  $\beta$ -cell action potentials and/or in regulation of insulin secretion. Inhibition of the repolarizing  $\text{K}^+$  currents the  $\text{K}_v$  channels generate augments insulin secretion.  $\text{K}_v1.4$ ,  $\text{K}_v1.5$ ,  $\text{K}_v2.1$ ,  $\text{K}_v2.2$ ,  $\text{K}_v3.1$ , and  $\text{K}_v3.2$   $\alpha$  subunits have been detected in the insulin-secreting cell line INS-1. Their inhibition by classic  $\text{K}_v$  channel blockers 4-aminopyridine, tetraethylammonium, and tetrapentyl ammonium enhanced tolbutamide-stimulated insulin secretion but not basal insulin secretion (11). Interestingly,  $\text{K}_v2.1$  directly interacts with the exocytotic machinery of  $\beta$  cells *via* syntaxin 1A, and this activity was recently postulated to be more important than its electrical activity in terms of effects on insulin secretion (12–14). Inhibition of  $\text{K}_v2.1$  has been suggested as a potential therapy for T2DM (15). Selective *KCNQ1* inhibition using chromanol 293B also augments glucose-stimulated insulin secretion from INS-1 cells (16) and mouse  $\beta$  cells *in vivo* and *ex vivo* (17).

*KCNQ1*,  $\text{K}_v1.4$ ,  $\text{K}_v1.5$ ,  $\text{K}_v2.1$ ,  $\text{K}_v3.1$ , and  $\text{K}_v3.2$  are all known to be regulated by the *KCNE2* single transmembrane domain ion channel ancillary subunit (18–23). *KCNE2*, part of the 5-member *KCNE* gene family, is ubiquitously expressed both in excitable cells and in non-excitable secretory epithelial cells; it can alter multiple facets of the  $\text{K}_v$   $\alpha$  subunits it regulates, including voltage dependence and kinetics of gating, trafficking, regulation by other factors, and pharmacology (24, 25). We previously found that *Kcne2* deletion impairs glucose tolerance of mice (26), but we did not explore the underlying mechanisms or pancreatic functions of *KCNE2*. We therefore investigated the potential role of *KCNE2* in pancreatic physiology and dysfunction.

## MATERIALS AND METHODS

### Generation of mice and study protocol

All mice were housed in pathogen-free facilities, and the study was approved by the Animal Care and Use Committee, University of California, Irvine. Studies were performed during the light cycle and were carried out in strict accordance with the recommendations in the *Guide for the Care and Use of Laboratory Animals* (National Institutes of Health, Bethesda, MD, USA). The *Kcne2*<sup>-/-</sup> mouse line was generated as previously described (27). Mice used in this study were bred by crossing *Kcne2*<sup>+/-</sup> mice that had been backcrossed >10 times into the C57BL/6 strain. After being genotyped and weaned at 3 wk of age, mice pups were assigned to, and maintained on, either a

control diet (2020X; Harlan Industries, Indianapolis, IN, USA; 16% kcal from fat, 19.1% protein, 2.7% crude fiber, 12.3% neutral detergent fiber, and 0% cholesterol) or Western diet (TD.88137; Harlan Industries; 42% kcal from fat, >60% of which is saturated; 34% sucrose; 0.2% cholesterol). All mice were subjected to glucose tolerance tests, preceded by 6 h food withdrawal, every 2 wk. Some cohorts had food withheld an additional 20 to 24 h every 2 wk commencing the morning after glucose tolerance tests, between wk 5 through 15 to 17, with similar food withholding protocols for mice of each diet and genotype. Mouse tissue and blood serum were then collected for further analysis or stored at  $-80^\circ\text{C}$ .

### Human pancreas immunostaining

Human pancreas immunostaining was performed by the University of California, Los Angeles (UCLA; Los Angeles, CA, USA), Translational Pathology Core Laboratory. Human tissue was obtained under UCLA institutional review board protocol 11002504CR00005. Paraffin-embedded sections were cut at 4  $\mu\text{m}$  thickness. Paraffin was removed with xylene, and the samples were rehydrated through graded ethanol. Endogenous peroxidase activity was blocked with 3% hydrogen peroxide in methanol for 10 min. Heat-induced antigen retrieval was carried out for all sections in 0.01 M citrate buffer, pH 6.00, using a Biocare decloaker (Biocare Medical, Concord, CA, USA) at  $95^\circ\text{C}$  for 25 min. The slides were then incubated overnight at  $4^\circ\text{C}$  with rabbit polyclonal *KCNE2* (1/2000; Alomone Labs, Jerusalem, Israel) or goat polyclonal *KCNQ1* (1/50; Santa Cruz Biotechnology, Santa Cruz, CA, USA). Secondary antibody rabbit anti-goat was used for *KCNQ1* at 1/200 for a 30-min incubation. The signal was detected using the rabbit horseradish peroxidase EnVision Kit (K4003; Dako, Glostrup, Denmark) and visualized with the diaminobenzidine reaction. The slides were rinsed and incubated with rabbit polyclonal anti-insulin antibody at 1/500 (*KCNE2*/insulin, *KCNQ1*/insulin) for 1 h for double staining. The signal was detected using March 2 Rabbit AP polymer (Biocare Medical) and visualized with Ferangi blue chromogen (alkaline phosphatase) (Biocare Medical). The sections were counterstained with nuclear fast red, air dried, and coverslipped.

### Islet isolation

For islet cell isolation, a pancreas each from a *Kcne2*<sup>+/+</sup> mouse and a *Kcne2*<sup>-/-</sup> mouse were collected and prepared in parallel, with both being placed in vials of collagenase solution containing (mM) 2.25 (D)-glucose, 1.26  $\text{CaCl}_2$ , 0.49  $\text{MgCl}_2 \cdot 6\text{H}_2\text{O}$ , 0.41  $\text{MgSO}_4 \cdot 7\text{H}_2\text{O}$ , 5.3 KCl, 0.44  $\text{KH}_2\text{PO}_4$ , 4.2  $\text{NaHCO}_3$ , 137.9 NaCl, 0.34  $\text{Na}_2\text{HPO}_4$  (solution 1) with 0.1% collagenase P and 0.2% bovine serum albumin, and then the vials placed in a  $37^\circ\text{C}$  water bath. The vials were observed for 14 to 16 min and shaken every 2 min. The duration of the warm-up was dependent on the amount of tissue present. Afterward, the vials were centrifuged at 500 rpm for 8 min at  $4^\circ\text{C}$  to pellet the cells. The supernatant was removed, and the cells were filtered 3 times through cell strainers into 50-ml vials using solution 1. The cells were pelleted once more, 3 ml of solution 1 was added, and the mixture was added to 3 ml of Histopaque 1.100 (54% 1.119 density Histopaque, 46% 1.077 density Histopaque) in a 15 ml vial. The vials were then centrifuged for 18 min at 900 rpm at  $4^\circ\text{C}$ , as previously described (28).

### Whole-cell patch electrophysiologic recording

The  $\beta$ -cell  $\text{K}^+$  currents were recorded by patch-clamping in the whole-cell configuration using an Axopatch 200B

amplifier and pCLAMP 9 software (Molecular Devices, Sunnyvale, CA, USA). Patch electrodes (2–4 M $\Omega$ ) were loaded with intracellular solution containing (mM) 140 KCl, 1 MgCl<sub>2</sub>[H<sub>2</sub>O]<sub>6</sub>, 10 EGTA, 10 HEPES, and 5 MgATP (adjusted to pH 7.25 with KOH). Islet cells were perfused with an extracellular bath solution containing (mM) 20 (D)-glucose, 119 NaCl, 2 CaCl<sub>2</sub>[(H<sub>2</sub>O)<sub>6</sub>], 4.7 KCl, 10 HEPES, 1.2 MgSO<sub>4</sub>, and 1.2 KH<sub>2</sub>PO<sub>4</sub> (adjusted to pH 7.3 with NaOH). The  $\beta$  cells were identified on the basis of their morphology and response to glucose concentration.

### Insulin secretion by isolated pancreatic islets

After isolation, islet cells were immediately used for insulin secretion analysis. Cells (200  $\mu$ l per batch) were removed with a micropipette and divided into 2 vials. Two milliliters of 3 mM glucose Krebs-Ringer bicarbonate (KRB) solution containing (mM) 119 NaCl, 2 CaCl<sub>2</sub>[(H<sub>2</sub>O)<sub>6</sub>], 4.7 KCl, 10 HEPES, 1.2 MgSO<sub>4</sub>, and 1.2 KH<sub>2</sub>PO<sub>4</sub> (adjusted to pH 7.3 with NaOH) (presaturated in 5% CO<sub>2</sub> to buffer the cells) was added. The solution was centrifuged and the supernatant removed, leaving solely the cells. KRB medium (2 ml) was again added, and vials were incubated in a shaking water bath at 37°C. The vials were then removed, centrifuged at 1200 rpm for 0.5 to 1 min, and the supernatant removed. The cells were counted using trypan blue, and acridine orange and propidium iodide dye, to ensure that the same amounts of cells were being examined for each sample; if one had a substantially larger amount of cells present, then the solution was diluted to normalize the cell numbers between each genotype. For insulin secretion in response to glucose, 200  $\mu$ l of cell solution was mixed with 200  $\mu$ l of 0, 6, and 16 mM glucose KRB medium for 30 min at 37°C. The vials were then incubated for another 30 min at 37°C. The vials were centrifuged, and the supernatants were extracted and stored in a –80°C freezer pending analysis by ELISA according to manufacturer's instructions (EMD Millipore, Billerica, MA, USA). ELISA plates were analyzed using a VERSA max plate reader with a Soft-Max Pro 5.3 data system (Molecular Devices, Silicon Valley, CA, USA)

### RNA isolation and real-time quantitative PCR

Mice were humanely killed by CO<sub>2</sub> asphyxiation. Pancreas tissue was collected, followed by left ventricle perfusion with cold PBS. Gastric fundus tissue was then collected and washed with PBS to remove stomach contents. For islet and nonislet cells, pancreas samples were pooled from 4 mice, and islet cell isolation was performed using the protocol described above. RNA from gastric and pancreatic tissue was extracted using 1 ml of Trizol (Thermo Fisher Scientific, Waltham, MA, USA) per 100 mg of tissue and purified using the RNeasy Mini Kit (Qiagen, Germantown, MD, USA) according to the manufacturer's protocol. RNA samples with  $A_{260}/A_{280}$  absorbance ratios between 2.00 and 2.20 were used for further synthesis. A total of 100 ng to 1  $\mu$ g of RNA was used for cDNA synthesis (Quantitect Reverse Transcriptase; Qiagen) and stored at –20°C until use.

Primer pairs for target gene *Kcne2* (NCBI Gene ID: 246133) and *Gapdh* (NCBI Gene ID: 14433) produced amplicons of 175 and 123 bp, respectively. The real-time quantitative PCR (qPCR) primer sequences were as follows: *Kcne2*, forward 5'-CACATAGCCAAATTGACCCAG-3', and reverse 5'-GAACATGCCATCATCACCAT-3'; *Gapdh*, forward 5'-AGGTCGGTGTG-AACGGATTG-3'; and reverse 5'-TGTAGACCATGTAGTTGAGGTCA-3. Primers (0.05  $\mu$ M synthesis scale, HPLC purified) were acquired from Sigma-Aldrich (St. Louis, MO, USA). Real-time qPCR analysis was performed using the CFX Connect System, iTaq Universal SYBR Green Supermix (Bio-Rad,

Hercules, CA, USA), and 96-well clear plates. Thermocycling parameters were set according to the manufacturer's protocol for iTaq. Samples were run in triplicate as a quality control measure, and triplicates with a SD  $\geq$  0.6 were repeated. Melting curves were assessed for verification of a single product.  $\Delta\Delta C_q$  values were normalized to those obtained for the *Kcne2*<sup>+/+</sup> stomach tissue.

### Islet cell RNA isolation and whole-transcript microarray analysis

Mice were humanely killed by CO<sub>2</sub> asphyxiation. After pancreas tissue isolation, islet cells were isolated as described above. RNA from islet cells was extracted using Trizol (Thermo Fisher Scientific) and purified using the RNeasy Mini Kit (Qiagen) according to the manufacturer's protocol. RNA samples with  $A_{260}/A_{280}$  absorbance ratios between 2.00 and 2.20 were stored at –80°C until used for further synthesis. Reverse-transcribed cDNA was analyzed by "whole-transcript transcriptomics" with the GeneAtlas microarray system (Affymetrix, Santa Clara, CA, USA) following the manufacturer's protocols. MoGene 1.1 ST array strips (Affymetrix) were used to hybridize to newly synthesized single-stranded cDNA. Each array comprised 770,317 distinct 25 mer probes to probe an estimated 28,944 transcripts, with a median 27 probes per gene. Gene expression changes associated with *Kcne2* deletion were analyzed by Ingenuity Pathway Analysis (Qiagen) to identify biologic networks, pathways, processes, and diseases that were most highly represented in the islet cell differentially expressed genes (DEGs) identified. Expression changes of  $\geq$ 2-fold and  $P < 0.05$  were included in the analysis.

### Western blot analysis

For quantification of insulin receptor  $\beta$  (IR- $\beta$ ) protein expression, skeletal muscle tissue from *Kcne2*<sup>+/+</sup> and *Kcne2*<sup>-/-</sup> mice was homogenized using a dounce homogenizer with 5 ml ice-cold lysis buffer [150 mM NaCl, 10 mM Tris (pH 7.4), 1 mM EDTA, 1 mM EGTA, 1% Triton X-100, 0.5% Nonidet P-40, 100 mM NaF, and 10 mM sodium orthovanadate]. Fresh protease inhibitor mini tablets (Pierce, Rockford, IL, USA) was added for every 10 ml of lysis buffer. After homogenization, samples were kept on ice for 30 min, then centrifuged at 600 rpm for 20 min at 4°C. Supernatant was centrifuged again at 13,000 rpm for 45 min at 4°C, and the final lysate was then collected. For quantification of insulin receptor substrate 1 (IRS-1), skeletal muscle was homogenized using a dounce homogenizer with 2.5 ml ice-cold lysis buffer. Lysis buffer was composed of 20 mM Tris (pH 8.0), 137 mM NaCl, 2.7 mM KCl, 10 mM NaF, 1 mM MgCl, 1 mM Na<sub>3</sub>VO<sub>4</sub>, 10% glycerol, and 1% Triton X-100. Fresh protease inhibitor mini tablets (Pierce) were added for every 10 ml of lysis buffer. After homogenization, samples were kept rotating in 4°C for 1 h, then centrifuged at 12,000 rpm for 10 min at 4°C, and the final lysate was collected. Subsequent steps were identical for all samples. The final lysate was collected and protein concentration was quantified using BCA Protein Assay (Thermo Fisher Scientific). Samples of equal target protein concentration were separated on NuPAGE 4 to 12% Bis-Tris gels and transferred onto PVDF membranes. Primary IR- $\beta$  subunit and IRS-1 antibodies (EMD Millipore) were diluted 1:1000 in 5% milk in Tris-buffered saline with 1% Tween-20 (TBST) and incubated either at room temperature for 2 h or overnight in 4°C on a rocker. Glyceraldehyde-3-phosphate dehydrogenase (GAPDH) antibody (Abcam, Cambridge, MA, USA) was used as loading control in 1:1000 dilution. Secondary antibodies (Bio-Rad) were added at 1:5000 dilutions in 3% milk in TBST. Antibodies were incubated at room temperature on a rocker

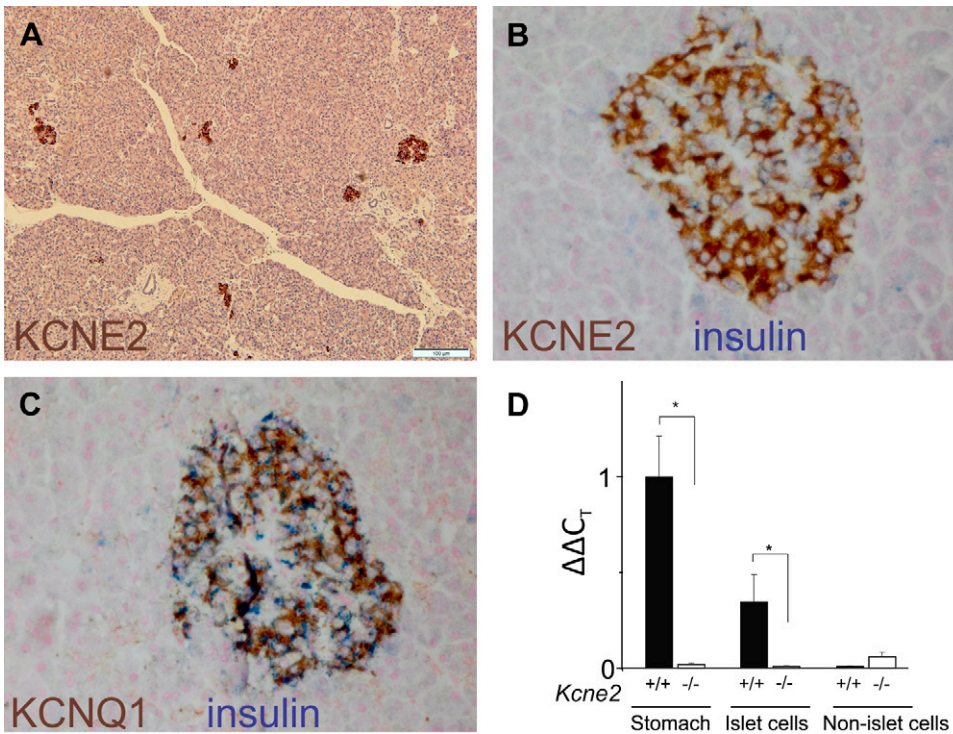


**Figure 1.** KCNE2 is expressed in human and mouse islet cells. A) KCNE2 immunostaining (brown) in human pancreas. Scale bar, 100  $\mu$ m. B) KCNE2 immunostaining (brown) colocalizing with insulin (blue) in human pancreatic islet. C) KCNQ1 immunostaining (brown) colocalizing with insulin (blue) in human pancreatic islet. D) *Kcne2* transcript expression quantified by qPCR in *Kcne2*<sup>+/+</sup> vs. *Kcne2*<sup>-/-</sup> mouse pancreas islet cells, nonislet cells, and stomach tissue for comparison. Data are means of  $n = 6$  independent measurements per group. Each independent measurement was itself mean of triplicate quantifications from cells isolated from 4 mice and pooled (total of 24 mice per group).

for 1 to 2 h. Membranes were then exposed to horseradish peroxidase substrate (EMD Millipore) for 5 min at room temperature, and chemiluminescence was visualized with on a Gbox system (Syngene, Frederick, MD, USA). Images were saved and analyzed with ImageJ software (Image Processing and Analysis in Java; National Institutes of Health, Bethesda, MD, USA; <http://imagej.nih.gov/>).

### Glucose tolerance test

Glucose tolerance tests were performed every 2 wk after weaning. Mice were injected intraperitoneally with 20% glucose in 0.9% NaCl solution (2 g of glucose/kg body weight) after withholding food for 6 hr. Blood samples were taken *via* tail vein before injection as well as 15, 30, 60, 90, and 120 min after injection for determination of blood glucose metabolism. Blood glucose in tail-vein blood samples was quantified using OneTouch Ultra glucose monitors (LifeScan, Milpitas, CA, USA). The corresponding relative area under the curve for glucose concentration was calculated using the trapezoid rule.

### Statistical analysis

Statistical analyses (Student's *t* test or ANOVA, as indicated in the figure captions) were performed assuming significance with a value of  $P < 0.05$ . Bonferroni and Holm corrections were used for multiple comparisons.

## RESULTS

### KCNE2 is expressed in human and mouse $\beta$ cells

KCNE2 protein was robustly expressed in human pancreatic islets, identified by insulin costaining; KCNQ1 exhibited a similar expression pattern (Fig. 1A–C). We

previously also detected *Kcne2* transcript expression in mouse pancreas by qPCR (26). Here, we discovered that pancreatic *Kcne2* transcript is expressed exclusively in mouse pancreas islet cells and is undetectable in pancreatic nonislet cells (Fig. 1D). Islet KCNE2 expression level was one third that measured in the stomach (Fig. 1D), where KCNE2 is known to be highly expressed (27).

### *Kcne2* deletion causes T2DM in mice

We previously detected glucose intolerance in adult *Kcne2*<sup>-/-</sup> mice fed normal mouse chow, but we did not pursue the mechanism in that study (26). Here, feeding with a Western diet had a dramatic effect on glucose tolerance of *Kcne2*<sup>-/-</sup> pups, causing glucose intolerance within 2 wk after weaning (by 5 wk of age), *vs.* no effect in *Kcne2*<sup>+/+</sup> pups at this age (Fig. 2A). By 21 wk, after 18 wk on the Western diet, *Kcne2*<sup>-/-</sup> mice were diabetic (baseline serum concentration of >200 mg/dl, and serum glucose concentration of >400 mg/dl measured 2 h after injection), whereas *Kcne2*<sup>+/+</sup> mice were only moderately less glucose tolerant than those on a control diet (Fig. 2B). All subsequent experiments in this study utilized adult mice fed regular mouse chow. Given the severity of effects of *Kcne2* deletion on glucose tolerance, we tested for hallmarks of T2DM in *Kcne2*<sup>-/-</sup> mice. Decreased skeletal muscle expression of IR- $\beta$  and IRS-1 is indicative of insulin resistance and characteristic of T2DM (29, 30). Here, using Western blot analyses, we demonstrated that *Kcne2* deletion decreases IR- $\beta$  and IRS-1 expression 2-fold in skeletal muscle (Fig. 2C, D).

We also performed microarray analysis of the islet cell transcriptomes of *Kcne2*<sup>+/+</sup> and *Kcne2*<sup>-/-</sup> mice. From a total of 28,944 gene transcripts, 1426 were found to be differentially expressed between female *Kcne2*<sup>-/-</sup> and *Kcne2*<sup>+/+</sup> mice using default filter criteria:

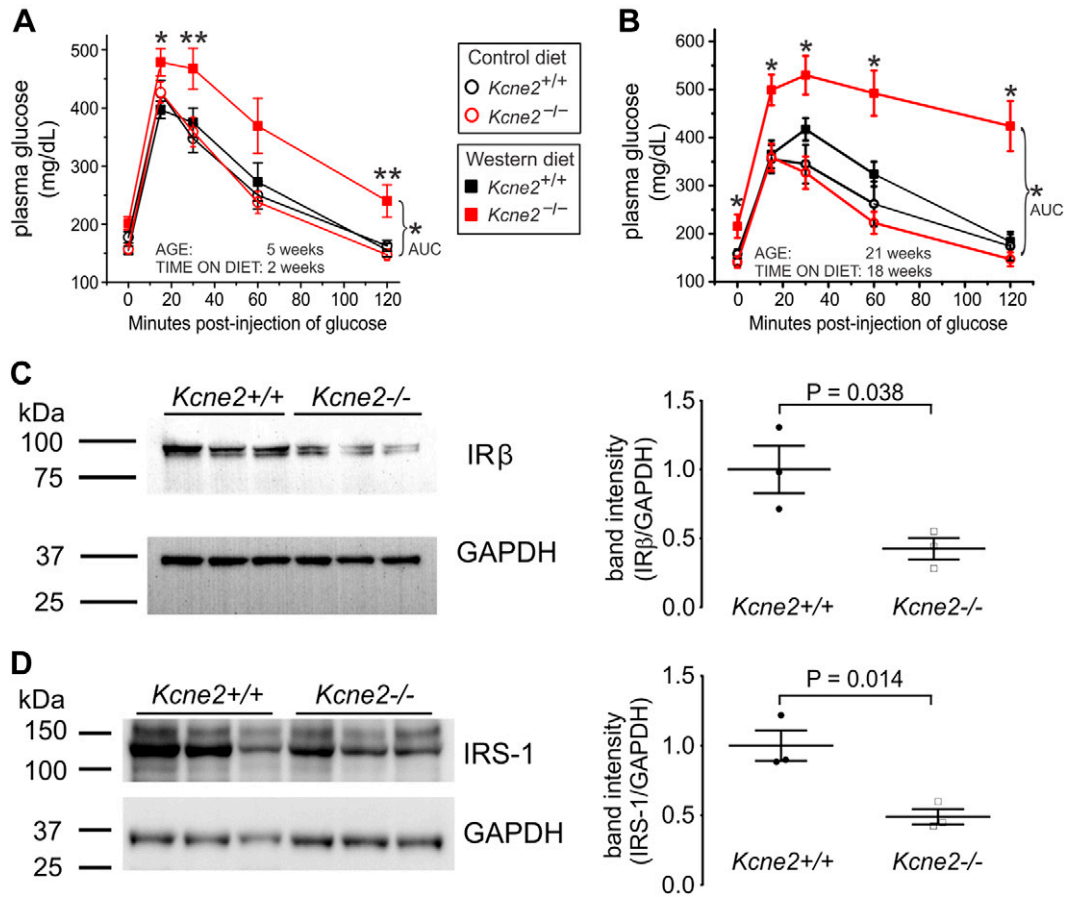


**Figure 2.** *Kcne2* deletion causes Western diet-exacerbated glucose intolerance and reduces insulin sensitivity. **A**) Glucose tolerance tests in 5-wk-old pups fed control or Western diet for 2 wk. \* $P < 0.05$ , \*\* $P < 0.01$  for Western diet-fed *Kcne2*<sup>-/-</sup> mice compared to all other groups (area under curve, AUC). Values are expressed as mean  $\pm$  SEM;  $n = 14$ –18 per group. **B**) As in **A**, but for 21-wk-old mice fed control or Western diet for 18 wk;  $n = 8$ –11. **C**, **D**) Left: Western blots of *Kcne2*<sup>+/+</sup> ( $n = 3$ ) and *Kcne2*<sup>-/-</sup> ( $n = 3$ ) mouse skeletal muscle lysates showing expression of IR- $\beta$  (**C**) and IRS-1 (**D**), with GAPDH as loading control (each lane using lysate from different mouse). Right: mean GAPDH-normalized band intensities quantified from blots on left. Error bars = SEM.

fold change (linear)  $< -2$  or  $< 2$ , and ANOVA  $P < 0.05$ . A total of 653 genes were up-regulated and 773 genes down-regulated in *Kcne2*<sup>-/-</sup> compared to *Kcne2*<sup>+/+</sup> mice. The transcriptome changes in *Kcne2*<sup>-/-</sup> mice were highly consistent with T2DM and included altered expression of T2DM markers, and gene expression changes indicative of islet cell proliferation, endoplasmic reticulum (ER) stress, increased ATP synthesis, and inflammation (**Fig. 3**). Furthermore, pathway analysis of islet cell *Kcne2* deletion-associated DEG networks showed changes highly consistent with T2DM, including islet cell proliferation (networks associated with protein synthesis and metabolism; Supplemental Fig. 1) and ER stress (EIF2 and EIF4 signaling pathways were the top 2 canonical signaling pathways activated; Supplemental Fig. 2). In addition, gene networks associated with amyloid precursor protein (APP; **Fig. 4**) and ERK signaling (Supplemental Fig. 3) were notably altered in *Kcne2*<sup>-/-</sup> mice.

### ***Kcne2* deletion impairs insulin secretion and alters $\beta$ -cell $K^+$ currents**

Crucially, germ-line *Kcne2* deletion resulted in dramatically impaired glucose-stimulated insulin secretion by

$\beta$  cells freshly isolated from mouse pancreas. The  $\beta$  cells isolated from 3- to 5-mo-old mice showed a *Kcne2* deletion-dependent 8-fold lower insulin secretion in response to 9.5 mM glucose, and lesser insulin secretion deficits at baseline and 4.5 mM glucose (**Fig. 5**).

Finally, we examined the effects of *Kcne2* deletion on freshly isolated  $\beta$ -cell  $K^+$  currents using whole-cell patch clamp. Peak outward current at +40 mV was 30% lower in  $\beta$  cells isolated from 3- to 6-mo-old *Kcne2*<sup>-/-</sup> mice compared to those from age-matched *Kcne2*<sup>+/+</sup> mice, but *Kcne2* deletion also produced a crossover of the  $I$ - $V$  relationships at -10 to -30 mV because of a left shift in the voltage dependence of the  $K^+$  current in this range (**Fig. 6A–C**). This left shift, of about 10 mV, was also apparent from normalized tail current-voltage relationships (**Fig. 6D, E**). In  $\beta$  cells isolated from 10- to 13-mo-old mice, current densities were lower than in  $\beta$  cells isolated from same-genotype 3 to 6 mo old mice, but *Kcne2* deletion had an even greater effect on peak  $K^+$  current than in younger mice, diminishing it by 45% at +40 mV (**Fig. 7A, B**). *Kcne2* deletion in older mice again resulted in a left shift of voltage dependence to whole-cell  $K^+$  current, this time in the wider range of -10 to -80 mV (**Fig. 7B, C**). Interestingly, *Kcne2* deletion reduced the amount of current decay

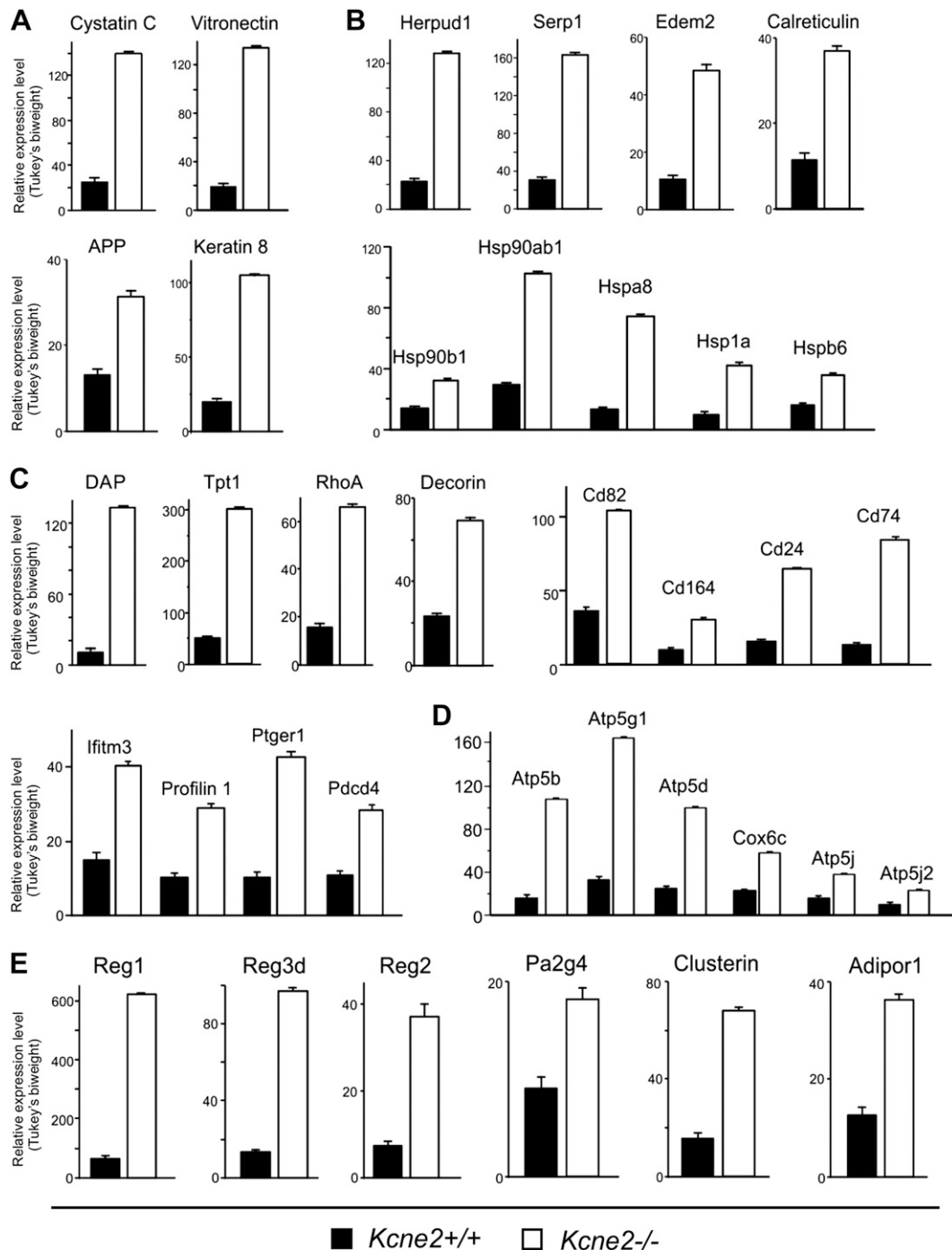


**Figure 3.** *Kcne2* deletion causes concerted islet cell transcriptomic changes characteristic of T2DM. Graphs show Tukey biweight signals of DEGs (quantified by microarray analysis; all changes shown reached  $P < 0.05$  significance level;  $n = 4$  mice per group) in islet cells isolated from 6-mo-old *Kcne2*<sup>+/+</sup> (solid columns) and *Kcne2*<sup>-/-</sup> mice (open columns). **A)** *Kcne2* deletion alters expression of known T2DM marker genes. **B)** *Kcne2* deletion causes transcript expression changes consistent with islet ER stress. **C)** *Kcne2* deletion causes transcript expression changes consistent with islet inflammation. **D)** *Kcne2* deletion increases islet expression of mitochondrial ATP synthesis-related genes. **E)** *Kcne2* deletion increases expression of proliferation-related genes in islets.

during depolarizing pulses only in 10- to 13- mo-old mice (Fig. 7D).

## DISCUSSION

*Kcne2* is widely expressed in mammalian tissues and is associated with a variety of disease states in both humans and mice. The promiscuity of KCNE2 makes defining its

exact physiologic roles and the molecular etiology of its associated disease states quite challenging (25). Human *KCNE2* polymorphisms within the coding region are associated with inherited and acquired (drug-induced) long QT syndrome, with the primary mechanism probably being direct disruption of  $K^+$  currents generated by *KCNE2* and various ventricular myocyte  $K_v$  channels with which it forms heteromeric complexes, the prime

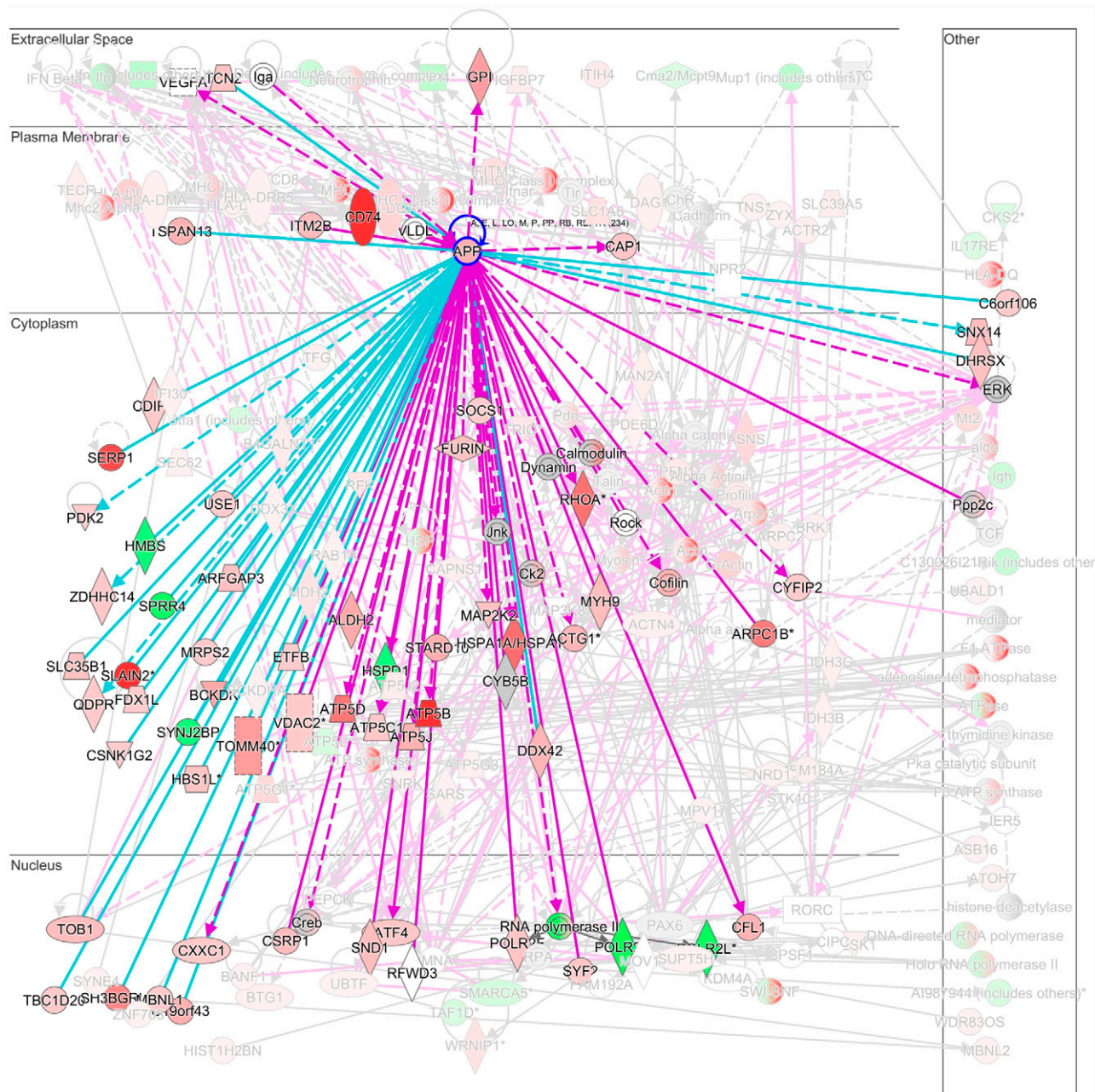


**Figure 4.** *Kcne2* deletion alters APP signaling network in islet cells. Pathway analysis of DEGs in *Kcne2*<sup>-/-</sup> vs. *Kcne2*<sup>+/+</sup> islet cells revealed one supernetwork of 6 connected networks, shown here. DEG with most connections within 6 networks was APP (highlighted). Solid lines: direct interactions; dashed lines: indirect interactions. For key to symbols, see Supplemental Fig. 1.

candidates being hERG and K<sub>v</sub>4.2/3 (22, 31–34). We recently found that *Kcne2* deletion causes atherosclerosis in mice, mirroring genome-wide association studies of human populations (35). *Kcne2*<sup>-/-</sup> mice also exhibit hypercholesterolemia, hypokalemia, and NAFLD as part of a multisystem syndrome (26, 36). Further, they exhibit increased susceptibility to stringent ischemia/reperfusion-induced sudden cardiac death (26), yet in cases of less stringent induced ischemia/reperfusion injury, they paradoxically exhibit less cardiac tissue damage because of chronic up-regulation of cardioprotective pathways involving GSK-3 $\beta$  inactivation (37).

The NAFLD in *Kcne2*<sup>-/-</sup> mice arises at least in part from iron deficiency caused by achlorhydria, which in turn arises because KCNE2-KCNQ1 channels are required for normal function of the gastric parietal cell H<sup>+</sup>/K<sup>+</sup>-ATPase that acidifies the stomach lumen (27, 36). In addition, KCNE2-KCNQ1 channels are required for efficient functioning of the sodium/iodide symporter in thyroid epithelial cells; thus, *Kcne2* deletion also causes hypothyroidism in pregnant and lactating dams, and in their pups (38). By adulthood, nongestating/lactating *Kcne2*<sup>-/-</sup> mice are euthyroid but can begin to show further signs of hypothyroidism at advanced age (>1 yr).

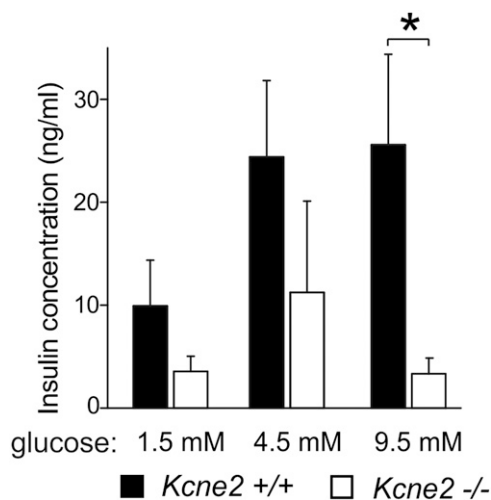


**Figure 5.** *Kcne2* deletion impairs glucose-stimulated insulin secretion by isolated  $\beta$  cells. Mean insulin secretion from islet  $\beta$  cells (incubated in buffer containing 1.5, 4.5, or 9.5 mM D-glucose) isolated from 3- to 4-mo-old *Kcne2*<sup>+/+</sup> and *Kcne2*<sup>-/-</sup> mice ( $n = 5$  mice per genotype). Error bars = SEM. \* $P < 0.05$ .

We also previously found that *Kcne2*<sup>-/-</sup> mice are glucose intolerant and deficient in regulating glucose levels after withholding food (26), but we did not pursue the mechanism until now. Despite the wide range of tissue defects caused by *Kcne2* deletion, in the current study, we have been able to establish that *Kcne2*<sup>-/-</sup> mice become diabetic as young adults when on a Western diet, and that *Kcne2* deletion causes a primary defect in  $\beta$ -cell insulin secretion in mice fed regular mouse chow. Young adult *Kcne2*<sup>-/-</sup> mice exhibit classic signs of T2DM, including the combination of impaired insulin secretion by the pancreas and impaired insulin sensitivity of skeletal muscle, which together contribute to glucose intolerance. Microarray analysis of islet cells revealed that *Kcne2* deletion causes remodeling highly consistent with what is known of the molecular pathology of T2DM. We detected in *Kcne2*<sup>-/-</sup> mice islet cells changes in the transcripts and/or signaling networks of a number of markers of T2DM, including cystatin C (39) and APP (40) (Figs. 3A and 4). ER stress, transcriptomic signatures for which were prominent in the islet cells of *Kcne2*<sup>-/-</sup> mice (Fig. 3B and Supplemental Fig. 2), results from glucolipotoxicity and is considered to be one of the main mechanisms underlying  $\beta$ -cell failure in T2DM (41–44). Detection of the EIF2 pathway as the predominant canonical signaling pathways altered in islet cells of *Kcne2*<sup>-/-</sup> mice is highly consistent with its known role in islet cell ER stress and islet cell development, physiology, and survival (45), and identification of EIF4-related signaling as the second highest altered pathway is also of interest with respect to  $\beta$ -cell function (46). Inflammation, also suggested by transcript expression changes in our microarray data (Fig. 3C), is another source of  $\beta$ -cell dysfunction in T2DM (47); the same applies to mitochondrial dysfunction (Fig. 3D) (43). Hyperproliferation, transcript changes associated with which we also detected in *Kcne2*<sup>-/-</sup> islets (Fig. 3E

and Supplemental Fig. 1), is also characteristic of T2DM (48).

The  $\beta$  cells from young adult *Kcne2*<sup>-/-</sup> mice exhibit a  $K^+$  current signature distinct from that of their wild-type littermates, with reduced peak currents at depolarized potentials but relatively more current at mildly negative potentials. Interestingly, we show for the first time, to our knowledge, that aging of mice (to 10–13 mo) reduces  $\beta$ -cell  $K^+$  current density even in wild-type mice, and that this is further diminished in *Kcne2*<sup>-/-</sup> mice.

The  $K^+$  current changes are suggestive of two events. First, we speculate that the reduced peak current at depolarized potentials arises from loss of KCNE2 from complexes with one or more of the various  $K_v$  channel  $\alpha$  subunits that are both expressed in islet cells and known to be up-regulated by KCNE2. One possible candidate is  $K_v1.5$ , given that KCNE2 increases  $K_v1.5$  activity 2-fold *in vitro*, *Kcne2* deletion decreases  $K_v1.5$  current  $\sim$ 2-fold in mouse ventricular myocytes (22), and  $K_v1.5$  is expressed in  $\beta$  cells (49). Another candidate would be  $K_v2.1$ ; however, we previously found that KCNE2 coexpression inhibits  $K_v2.1$  *in vitro* and reduces its inactivation (21), so this does not match with our  $\beta$ -cell data (which shows similar effects, but for deletion of KCNE2, not addition). It is possible that  $K_v2.1$  forms complexes with, for example,  $K_v2.2$  in  $\beta$  cells, and that these heteromers are differentially affected by KCNE2. Second, we suggest that the relative increase in  $K^+$  current at mildly hyperpolarized potentials arises at least partly from loss of KCNE2 from complexes with KCNQ1. Although coassembly with KCNE2 converts KCNQ1 to a channel with left-shifted voltage dependence, able to remain constitutively open at resting membrane potentials, KCNE2 reduces KCNQ1 current magnitude 2- to 3-fold between  $-50$  and  $0$  mV (23). KCNE2 coexpression *in vitro* also inhibits  $K_v2.1$ , as mentioned above, and so removal of this inhibition could also contribute; however,  $K_v2.1$  activates  $\sim$ 10 to 20 mV more positively than KCNQ1 (in our hands), and so increased  $K_v2.1$  current would not explain the current increase in  $\beta$  cells from *Kcne2*<sup>-/-</sup> mice across the voltage range that we observed ( $-80$  to  $-10$  mV in 10–13 mo-old adult mice). At this stage, the technical difficulties encountered in isolating sufficient  $\beta$  cells, maintaining them in healthy condition, and recording from them has limited our analyses to defining the changes in whole-cell current associated with *Kcne2* deletion, but future analyses may involve identification of the specific  $K_v$   $\alpha$  subunits affected.

Previous studies showed that pharmacologic inhibition of  $K_v1.5$  or  $K_v2.1$  increased insulin secretion and also diminished  $\beta$ -cell apoptosis (11). Likewise, inhibition of KCNQ1 with chromanol 293B enhanced glucose-stimulated insulin secretion in mice and in INS-1 cells (16, 17). Germ-line deletion of *Kcnq1* in mice was previously found to enhance insulin sensitivity in the liver (50), but recently to not alter insulin secretion from pancreatic islets (51). However, *Kcnq1* deletion did impair glucose tolerance and reduce  $\beta$ -cell mass when parental origin of the null allele was taken into account, and was associated with paternal heterozygous transmission. This was deduced to arise from loss of imprinting control and associated epigenetic modification

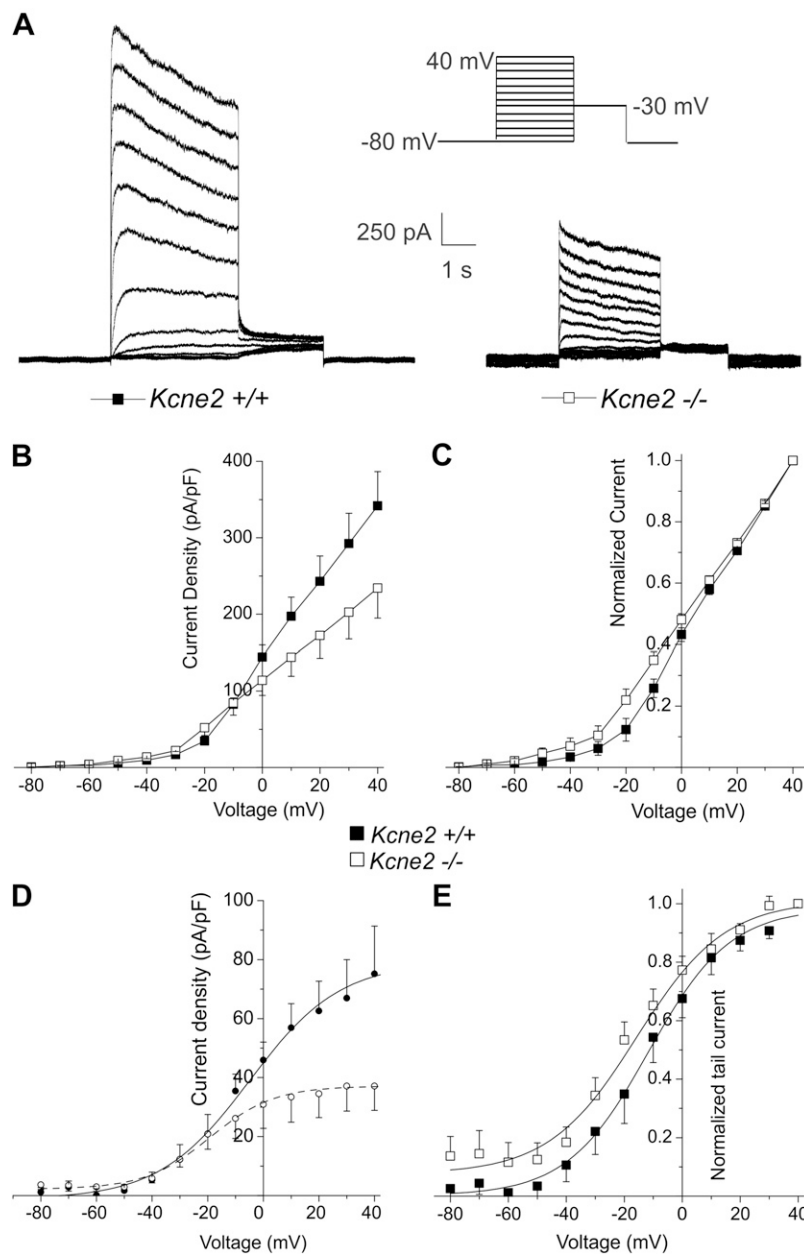


**Figure 6.** *Kcne2* deletion alters delayed rectifier  $K^+$  currents in  $\beta$  cells isolated from young adult mice. **A)** Exemplar current traces recorded in response to 4-s depolarizations in 10-mV increments from  $-80$  to  $+40$  mV in islet  $\beta$  cells from 3- to 5-mo-old *Kcne2*<sup>+/+</sup> ( $n = 9$ ) and *Kcne2*<sup>-/-</sup> ( $n = 8$ ) mice. **B, C)** Mean raw current-voltage relationship (**B**) and normalized current-voltage relationship (**C**) from cells as in **A** ( $n = 8$ –9 cells from 4 mice). Error bars = SEM. **D, E)** Mean raw (**D**) and normalized (**E**)  $-30$  mV tail current vs. prepulse voltage relationship for cells as in **A** ( $n = 8$ –9 cells from 4 mice). Error bars = SEM.

of neighboring gene *Cdkn1c*. This is because the *Kcnq1* gene is overlapped by the noncoding RNA *KCNQ1* overlapping transcript (*Kcnq1ot1*), which regulates neighboring genes on the paternal allele. For this reason, it has been very difficult to ascertain the mechanisms underlying the mechanisms by which *KCNQ1* regulates pancreatic function and diabetes *via* its role as an ion channel or otherwise.

Our finding that *Kcne2* deletion impairs insulin secretion and insulin sensitivity tallies well with a role for KCNE2-KCNQ1 complexes in regulating insulin secretion, as by enhancing *KCNQ1* currents in the moderately hyperpolarized range, we would be predicted to obtain results opposite to pharmacologic inhibition of *KCNQ1*, which we did. If a role for KCNE2-KCNQ1 complexes in regulation of insulin secretion is further supported in future studies, it could have important

implications for new therapeutic avenues and for avoidance of side effects if targeting *KCNQ1* channels in other tissues, given that each *KCNE* isoform lends specific attributes to *KCNQ1* pharmacology (52–54). Interestingly,  $I_{KS}$  channels, formed by *KCNQ1* and *KCNE1*, are activated by increased intracellular ATP, independent of the augmenting effects of  $PIP_2$  on *KCNQ1* (55). This effect is opposite to that of  $K_{ATP}$  channels, which are inhibited by ATP to trigger the cascade of events that induces insulin secretion. Therefore, we hypothesize that *KCNE2-KCNQ1* channels in  $\beta$  cells provide a brake to prevent excessive insulin secretion and help return  $\beta$  cells to resting membrane potential. By deleting *Kcne2*, we may have increased the activity of this brake at mildly negative potentials, to the extent that insulin secretion is impaired. This hypothesis would also fit with previous

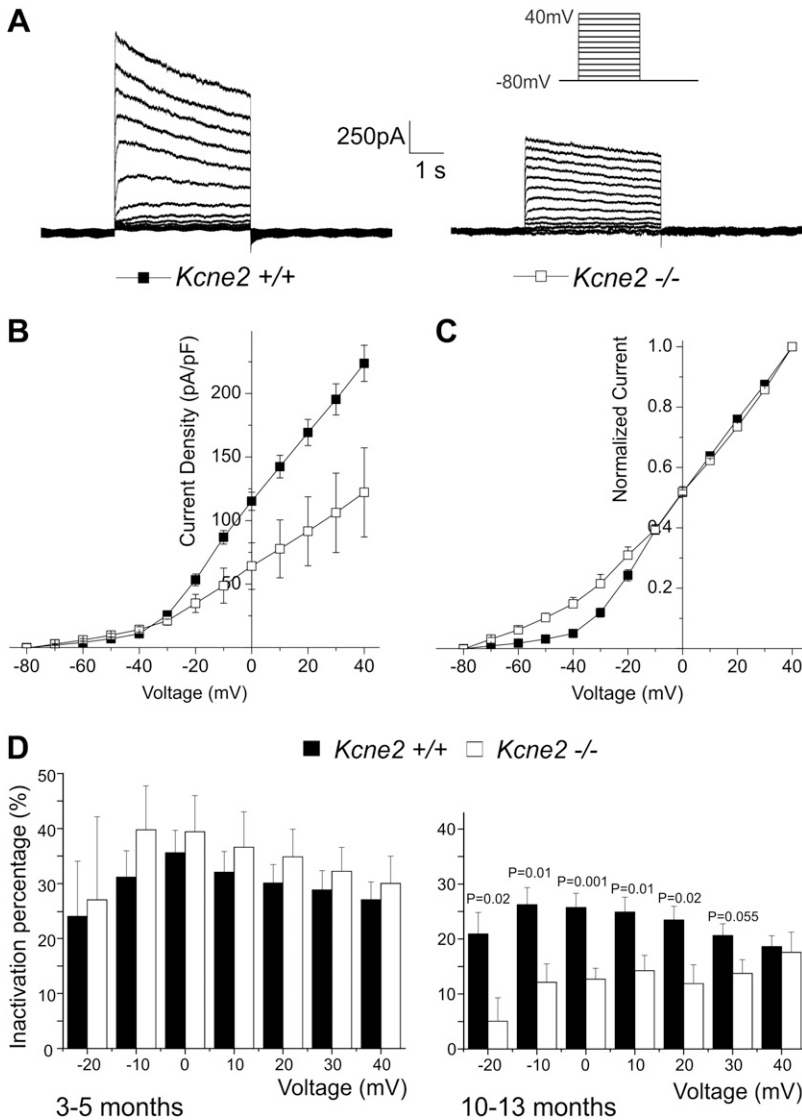


**Figure 7.** Aging and *Kcne2* deletion alters delayed rectifier  $K^+$  currents in  $\beta$  cells isolated from older adult mice. **A)** Exemplar current traces recorded in response to 4-s depolarizations in 10-mV increments from  $-80$  to  $+40$  mV (upper right inset: voltage protocol) in islet  $\beta$  cells from 10- to 13-mo-old *Kcne2*<sup>+/+</sup> ( $n = 15$ ) and *Kcne2*<sup>-/-</sup> ( $n = 7$ ) mice. **B, C)** Mean raw current-voltage relationship (**B**) and normalized current-voltage relationship (**C**) from cells as in **A** ( $n = 7$ –15 cells from 4 mice). Error bars = SEM. **D)** Mean percentage decay (inactivation) over 4 s of  $K^+$  currents recorded as in **A** from 3- to 5-mo-old (left) and 10- to 13-mo-old (right) *Kcne2*<sup>+/+</sup> and *Kcne2*<sup>-/-</sup> mice ( $n = 7$ –15 cells from 4 mice).

findings that inhibition of KCNQ1 increases insulin secretion (17) and that overexpression of KCNQ1 in the MIN6  $\beta$ -cell line impairs insulin secretion (56). **FJ**

G. W. Abbott performed critical revision of the article for important intellectual content.

## ACKNOWLEDGMENTS

This work was supported by University of California, Irvine setup funds (to G.W.A.). The authors gratefully acknowledge H. Ishii (University of California, Irvine) for helpful technical advice, and N. B. Doan (University of California, Los Angeles, Los Angeles, CA, USA) for performing human pancreas immunostaining.

## AUTHOR CONTRIBUTIONS

S. M. Lee, Z. Hu, and G. W. Abbott designed the research study; S. M. Lee, S. Liu, D. Nguyen, J. Baik, V. Nguyen, Z. Hu, and G. W. Abbott conducted the experiments; S. M. Lee, S. Liu, D. Nguyen, J. Baik, V. Nguyen, and G. W. Abbott analyzed the data; G. W. Abbott drafted the article and obtained the funding; and S. M. Lee, D. Nguyen, and

## REFERENCES

- DeFronzo, R. A., and Ferrannini, E. (1991) Insulin resistance. A multifaceted syndrome responsible for NIDDM, obesity, hypertension, dyslipidemia, and atherosclerotic cardiovascular disease. *Diabetes Care* **14**, 173–194
- Yasuda, K., Miyake, K., Horikawa, Y., Hara, K., Osawa, H., Furuta, H., Hirota, Y., Mori, H., Jonsson, A., Sato, Y., Yamagata, K., Hinokio, Y., Wang, H. Y., Tanahashi, T., Nakamura, N., Oka, Y., Iwasaki, N., Iwamoto, Y., Yamada, Y., Seino, Y., Maegawa, H., Kashiwagi, A., Takeda, J., Maeda, E., Shin, H. D., Cho, Y. M., Park, K. S., Lee, H. K., Ng, M. C., Ma, R. C., So, W. Y., Chan, J. C., Lyssenko, V., Tuomi, T., Nilsson, P., Groop, L., Kamatani, N., Sekine, A., Nakamura, Y., Yamamoto, K., Yoshida, T., Tokunaga, K., Itakura, M., Makino, H., Nanjo, K., Kadowaki, T., and Kasuga, M. (2008) Variants in *KCNQ1* are associated with susceptibility to type 2 diabetes mellitus. *Nat. Genet.* **40**, 1092–1097
- Virkamäki, A., Ueki, K., and Kahn, C. R. (1999) Protein-protein interaction in insulin signaling and the molecular mechanisms of insulin resistance. *J. Clin. Invest.* **103**, 931–943
- Warram, J. H., Martin, B. C., Krolewski, A. S., Soeldner, J. S., and Kahn, C. R. (1990) Slow glucose removal rate and hyperinsulinemia precede

- the development of type II diabetes in the offspring of diabetic parents. *Ann. Intern. Med.* **113**, 909–915
5. Olefsky, J. M., and Nolan, J. J. (1995) Insulin resistance and non-insulin-dependent diabetes mellitus: cellular and molecular mechanisms. *Am. J. Clin. Nutr.* **61**(4, Suppl)980S–986S
  6. Chiasson, J. L., and Rabasa-Lhoret, R. (2004) Prevention of type 2 diabetes: insulin resistance and beta-cell function. *Diabetes* **53**(Suppl 3), S34–S38
  7. Gerich, J. E. (1999) Is insulin resistance the principal cause of type 2 diabetes? *Diabetes Obes. Metab.* **1**, 257–263
  8. Tucker, S. J., Gribble, F. M., Zhao, C., Trapp, S., and Ashcroft, F. M. (1997) Truncation of Kir6.2 produces ATP-sensitive K<sup>+</sup> channels in the absence of the sulphonylurea receptor. *Nature* **387**, 179–183
  9. Nichols, C. G., and Koster, J. C. (2002) Diabetes and insulin secretion: whither KATP? *Am. J. Physiol. Endocrinol. Metab.* **283**, E403–E412
  10. Tarasov, A. I., Welters, H. J., Senkel, S., Ryffel, G. U., Hattersley, A. T., Morgan, N. G., and Ashcroft, F. M. (2006) A Kir6.2 mutation causing neonatal diabetes impairs electrical activity and insulin secretion from INS-1 beta-cells. *Diabetes* **55**, 3075–3082
  11. Su, J., Yu, H., Lenka, N., Hescheler, J., and Ullrich, S. (2001) The expression and regulation of depolarization-activated K<sup>+</sup> channels in the insulin-secreting cell line INS-1. *Pflügers Arch.* **442**, 49–56
  12. Dai, X. Q., Manning Fox, J. E., Chikvashvili, D., Casimir, M., Plummer, G., Hajmrle, C., Spigelman, A. F., Kin, T., Singer-Lahat, D., Kang, Y., Shapiro, A. M., Gaisano, H. Y., Lotan, I., and Macdonald, P. E. (2012) The voltage-dependent potassium channel subunit Kv2.1 regulates insulin secretion from rodent and human islets independently of its electrical function. *Diabetologia* **55**, 1709–1720
  13. Leung, Y. M., Kang, Y., Gao, X., Xia, F., Xie, H., Sheu, L., Tsuk, S., Lotan, I., Tsushima, R. G., and Gaisano, H. Y. (2003) Syntaxin 1A binds to the cytoplasmic C terminus of Kv2.1 to regulate channel gating and trafficking. *J. Biol. Chem.* **278**, 17532–17538
  14. MacDonald, P. E., Wang, G., Tsuk, S., Dodo, C., Kang, Y., Tang, L., Wheeler, M. B., Cattral, M. S., Lakey, J. R., Salapatek, A. M., Lotan, I., and Gaisano, H. Y. (2002) Synaptosome-associated protein of 25 kilodaltons modulates Kv2.1 voltage-dependent K(+) channels in neuroendocrine islet beta-cells through an interaction with the channel N terminus. *Mol. Endocrinol.* **16**, 2452–2461
  15. Li, X. N., Herrington, J., Petrov, A., Ge, L., Eiermann, G., Xiong, Y., Jensen, M. V., Hohmeier, H. E., Newgard, C. B., Garcia, M. L., Wagner, M., Zhang, B., Thornberry, N. A., Howard, A. D., Kaczorowski, G. J., and Zhou, Y. P. (2013) The role of voltage-gated potassium channels Kv2.1 and Kv2.2 in the regulation of insulin and somatostatin release from pancreatic islets. *J. Pharmacol. Exp. Ther.* **344**, 407–416
  16. Ullrich, S., Su, J., Ranta, F., Wittekindt, O. H., Ris, F., Rösler, M., Gerlach, U., Heitzmann, D., Warth, R., and Lang, F. (2005) Effects of I (Ks) channel inhibitors in insulin-secreting INS-1 cells. *Pflügers Arch.* **451**, 428–436
  17. Liu, L., Wang, F., Lu, H., Ren, X., and Zou, J. (2014) Chromanol 293B, an inhibitor of KCNQ1 channels, enhances glucose-stimulated insulin secretion and increases glucagon-like peptide-1 level in mice. *Islets* **6**, e962386
  18. Kanda, V. A., Lewis, A., Xu, X., and Abbott, G. W. (2011) KCNE1 and KCNE2 provide a checkpoint governing voltage-gated potassium channel  $\alpha$ -subunit composition. *Biophys. J.* **101**, 1364–1375
  19. Kanda, V. A., Lewis, A., Xu, X., and Abbott, G. W. (2011) KCNE1 and KCNE2 inhibit forward trafficking of homomeric N-type voltage-gated potassium channels. *Biophys. J.* **101**, 1354–1363
  20. Lewis, A., McCrossan, Z. A., and Abbott, G. W. (2004) MinK, MiRP1, and MiRP2 diversify Kv3.1 and Kv3.2 potassium channel gating. *J. Biol. Chem.* **279**, 7884–7892
  21. McCrossan, Z. A., Roepke, T. K., Lewis, A., Panaghie, G., and Abbott, G. W. (2009) Regulation of the Kv2.1 potassium channel by MinK and MiRP1. *J. Membr. Biol.* **228**, 1–14
  22. Roepke, T. K., Kontogeorgis, A., Ovanez, C., Xu, X., Young, J. B., Purtell, K., Goldstein, P. A., Christini, D. J., Peters, N. S., Akar, F. G., Gutstein, D. E., Lerner, D. J., and Abbott, G. W. (2008) Targeted deletion of *kcnk2* impairs ventricular repolarization via disruption of I (K<sub>slow</sub>) and I (to, f). *FASEB J.* **22**, 3648–3660
  23. Tinel, N., Diochot, S., Borsotto, M., Lazdunski, M., and Barhanin, J. (2000) KCNE2 confers background current characteristics to the cardiac KCNQ1 potassium channel. *EMBO J.* **19**, 6326–6330
  24. Abbott, G. W. (2012) KCNE2 and the K(+) channel: the tail wagging the dog. *Channels (Austin)* **6**, 1–10
  25. Abbott, G. W. (2015) The KCNE2 K<sup>+</sup> channel regulatory subunit: ubiquitous influence, complex pathobiology. *Gene* **569**, 162–172
  26. Hu, Z., Kant, R., Anand, M., King, E. C., Krogh-Madsen, T., Christini, D. J., and Abbott, G. W. (2014) *Kcne2* deletion creates a multisystem syndrome predisposing to sudden cardiac death. *Circ Cardiovasc Genet* **7**, 33–42
  27. Roepke, T. K., Anantharam, A., Kirchhoff, P., Busque, S. M., Young, J. B., Geibel, J. P., Lerner, D. J., and Abbott, G. W. (2006) The KCNE2 potassium channel ancillary subunit is essential for gastric acid secretion. *J. Biol. Chem.* **281**, 23740–23747
  28. Li, D. S., Yuan, Y. H., Tu, H. J., Liang, Q. L., and Dai, L. J. (2009) A protocol for islet isolation from mouse pancreas. *Nat. Protoc.* **4**, 1649–1652
  29. Caro, J. F., Sinha, M. K., Raju, S. M., Ittoop, O., Pories, W. J., Flickinger, E. G., Meelheim, D., and Dohm, G. L. (1987) Insulin receptor kinase in human skeletal muscle from obese subjects with and without noninsulin dependent diabetes. *J. Clin. Invest.* **79**, 1330–1337
  30. Kerouz, N. J., Hörsch, D., Pons, S., and Kahn, C. R. (1997) Differential regulation of insulin receptor substrates-1 and -2 (IRS-1 and IRS-2) and phosphatidylinositol 3-kinase isoforms in liver and muscle of the obese diabetic (ob/ob) mouse. *J. Clin. Invest.* **100**, 3164–3172
  31. Abbott, G. W., Sesti, F., Splawski, I., Buck, M. E., Lehmann, M. H., Timothy, K. W., Keating, M. T., and Goldstein, S. A. (1999) MiRP1 forms IKr potassium channels with HERG and is associated with cardiac arrhythmia. *Cell* **97**, 175–187
  32. Zhang, M., Jiang, M., and Tseng, G. N. (2001) minK-related peptide 1 associates with Kv4.2 and modulates its gating function: potential role as beta subunit of cardiac transient outward channel? *Circ. Res.* **88**, 1012–1019
  33. Isbrandt, D., Friederich, P., Solth, A., Haverkamp, W., Ebner, A., Borggrefe, M., Funke, H., Sauter, K., Breithardt, G., Pongs, O., and Schulze-Bahr, E. (2002) Identification and functional characterization of a novel KCNE2 (MiRP1) mutation that alters HERG channel kinetics. *J. Mol. Med. (Berl.)* **80**, 524–532
  34. Gordon, E., Panaghie, G., Deng, L., Bee, K. J., Roepke, T. K., Krogh-Madsen, T., Christini, D. J., Ostrer, H., Basson, C. T., Chung, W., and Abbott, G. W. (2008) A KCNE2 mutation in a patient with cardiac arrhythmia induced by auditory stimuli and serum electrolyte imbalance. *Cardiovasc. Res.* **77**, 98–106
  35. Lee, S. M., Nguyen, D., Hu, Z., and Abbott, G. W. (2015) *Kcne2* deletion promotes atherosclerosis and diet-dependent sudden death. *J. Mol. Cell. Cardiol.* **87**, 148–151
  36. Lee, S. M., Nguyen, D., Anand, M., Kant, R., Köhnke, C., Lisewski, U., Roepke, T. K., Hu, Z., and Abbott, G. W. (2016) *Kcne2* deletion causes early-onset nonalcoholic fatty liver disease via iron deficiency anemia. *Sci. Rep.* **6**, 23118
  37. Hu, Z., Crump, S. M., Zhang, P., and Abbott, G. W. (2016) *Kcne2* deletion attenuates acute post-ischaemia/reperfusion myocardial infarction. *Cardiovasc. Res.* **110**, 227–237
  38. Roepke, T. K., King, E. C., Reyna-Neyra, A., Paroder, M., Purtell, K., Koba, W., Fine, E., Lerner, D. J., Carrasco, N., and Abbott, G. W. (2009) *Kcne2* deletion uncovers its crucial role in thyroid hormone biosynthesis. *Nat. Med.* **15**, 1186–1194
  39. Reutens, A. T., Bonnet, F., Lantieri, O., Roussel, R., and Balkau, B.; Epidemiological Study on the Insulin Resistance Syndrome Study Group. (2013) The association between cystatin C and incident type 2 diabetes is related to central adiposity. *Nephrol. Dial. Transplant.* **28**, 1820–1829
  40. Westermark, P., Andersson, A., and Westermark, G. T. (2011) Islet amyloid polypeptide, islet amyloid, and diabetes mellitus. *Physiol. Rev.* **91**, 795–826
  41. Marcu, M. G., Doyle, M., Bertolotti, A., Ron, D., Hendershot, L., and Neckers, L. (2002) Heat shock protein 90 modulates the unfolded protein response by stabilizing IRE1 $\alpha$ . *Mol. Cell. Biol.* **22**, 8506–8513
  42. Ramos, R. R., Swanson, A. J., and Bass, J. (2007) Calreticulin and Hsp90 stabilize the human insulin receptor and promote its mobility in the endoplasmic reticulum. *Proc. Natl. Acad. Sci. USA* **104**, 10470–10475
  43. Back, S. H., and Kaufman, R. J. (2012) Endoplasmic reticulum stress and type 2 diabetes. *Annu. Rev. Biochem.* **81**, 767–793
  44. Eletto, D., Dersh, D., and Argon, Y. (2010) GRP94 in ER quality control and stress responses. *Semin. Cell Dev. Biol.* **21**, 479–485

45. Harding, H. P., and Ron, D. (2002) Endoplasmic reticulum stress and the development of diabetes: a review. *Diabetes* **51** (Suppl 3), S455–S461
46. Thierry, M., Pasquis, B., Buteau, B., Fourgeux, C., Dembele, D., Leclere, L., Gambert-Nicot, S., Acar, N., Bron, A. M., Creuzot-Garcher, C. P., and Bretillon, L. (2015) Early adaptive response of the retina to a pro-diabetogenic diet: impairment of cone response and gene expression changes in high-fructose fed rats. *Exp. Eye Res.* **135**, 37–46
47. Donath, M. Y., Böni-Schnetzler, M., Ellingsgaard, H., and Ehses, J. A. (2009) Islet inflammation impairs the pancreatic beta-cell in type 2 diabetes. *Physiology (Bethesda)* **24**, 325–331
48. Cerf, M. E. (2013) Beta cell dysfunction and insulin resistance. *Front. Endocrinol. (Lausanne)* **4**, 37
49. Kim, S. J., Ao, Z., Warnock, G., and McIntosh, C. H. (2013) Incretin-stimulated interaction between  $\beta$ -cell Kv1.5 and Kv $\beta$ 2 channel proteins involves acetylation/deacetylation by CBP/SirT1. *Biochem. J.* **451**, 227–234
50. Boini, K. M., Graf, D., Hennige, A. M., Koka, S., Kempe, D. S., Wang, K., Ackermann, T. F., Föller, M., Vallon, V., Pfeifer, K., Schleicher, E., Ullrich, S., Häring, H. U., Häussinger, D., and Lang, F. (2009) Enhanced insulin sensitivity of gene-targeted mice lacking functional *KCNQ1*. *Am. J. Physiol. Regul. Integr. Comp. Physiol.* **296**, R1695–R1701
51. Asahara, S., Etoh, H., Inoue, H., Teruyama, K., Shibusaki, Y., Ihara, Y., Kawada, Y., Bartolome, A., Hashimoto, N., Matsuda, T., Koyanagi-Kimura, M., Kanno, A., Hirota, Y., Hosooka, T., Nagashima, K., Nishimura, W., Inoue, H., Matsumoto, M., Higgins, M. J., Yasuda, K., Inagaki, N., Seino, S., Kasuga, M., and Kido, Y. (2015) Paternal allelic mutation at the *Kcnq1* locus reduces pancreatic  $\beta$ -cell mass by epigenetic modification of Cdkn1c. *Proc. Natl. Acad. Sci. USA* **112**, 8332–8337
52. Panaghie, G., and Abbott, G. W. (2006) The impact of ancillary subunits on small-molecule interactions with voltage-gated potassium channels. *Curr. Pharm. Des.* **12**, 2285–2302
53. Heitzmann, D., Grahammer, F., von Hahn, T., Schmitt-Gräff, A., Romeo, E., Nitschke, R., Gerlach, U., Lang, H. J., Verrey, F., Barhanin, J., and Warth, R. (2004) Heteromeric *KCNE2/KCNQ1* potassium channels in the luminal membrane of gastric parietal cells. *J. Physiol.* **561**, 547–557
54. Roura-Ferrer, M., Solé, L., Oliveras, A., Dahan, R., Bielanska, J., Villaruel, A., Comes, N., and Felipe, A. (2010) Impact of KCNE subunits on *KCNQ1* (Kv7.1) channel membrane surface targeting. *J. Cell. Physiol.* **225**, 692–700
55. Li, Y., Gao, J., Lu, Z., McFarland, K., Shi, J., Bock, K., Cohen, I. S., and Cui, J. (2013) Intracellular ATP binding is required to activate the slowly activating K<sup>+</sup> channel I(Ks). *Proc. Natl. Acad. Sci. USA* **110**, 18922–18927
56. Yamagata, K., Senokuchi, T., Lu, M., Takemoto, M., Fazlul Karim, M., Go, C., Sato, Y., Hatta, M., Yoshizawa, T., Araki, E., Miyazaki, J., and Song, W. J. (2011) Voltage-gated K<sup>+</sup> channel *KCNQ1* regulates insulin secretion in MIN6  $\beta$ -cell line. *Biochem. Biophys. Res. Commun.* **407**, 620–625

Received for publication December 15, 2016.  
Accepted for publication February 21, 2017.